Results in Physics 66 (2024) 108007

Contents lists available at ScienceDirect

Results in Physics

journal homepage: www.elsevier.com/locate/rinp

Time-dependent relaxation dynamics of remanent strain in textured PMN–PZ–PT and PMN–PIN–PT piezoceramics

Temesgen Tadeyos Zate [a,b], Astri Bjørnetun Haugen [a], Dariusz Mikielewicz [c], Jae-Ho Jeon [b,c,*]

[a] Department of Energy Conversion and Storage, Technical University of Denmark, Anker Engelundsvej, Building 301, 2800 Kgs Lyngby, Denmark
[b] Formerly with the Functional Powder Materials Department, Korea Institute of Materials Science, Changwondaero 797, Changwon 51508, Republic of Korea
[c] Faculty of Mechanical Engineering and Ship Technology, Gdansk University of Technology, 80-233 Gdansk, Poland

ARTICLE INFO

Keywords:
Textured piezoceramics
Embedded template
Remanent strain
Strain relaxation dynamics
Time delay

ABSTRACT

Crystallographically textured lead-based piezoceramics, particularly $Pb(Mg_{1/3}Nb_{2/3})O_3$–$PbZrO_3$–$PbTiO_3$ (PMN–PZ–PT) and $Pb(Mg_{1/3}Nb_{2/3})O_3$–$Pb(In_{1/2}Nb_{1/2})O_3$–$PbTiO_3$ (PMN–PIN–PT), play a pivotal role in electromechanical applications due to their enhanced field-induced strain responses. However, challenges in precision positioning arise from heightened remanent strain (S_r) caused by embedded templates in the textured grains, impacting strain cycle consistency due to increased time delay for S_r relaxation. This study investigates the time-dependent relaxation dynamics of S_r in textured PMN–PZ–PT and PMN–PIN–PT piezoceramics, focusing on experimentally determining relaxation time between cycles required for complete S_r relaxation. Our findings reveal that the relaxation time in textured piezoceramics is notably longer than that in their non-textured counterparts, primarily due to pinning of domain walls by embedded templates. This work provides insights into the strain relaxation characteristics of piezoceramics and underscores the importance of time delay in designing precision positioning systems for improved reliability.

Introduction

Piezoceramics with large unipolar strain response and consistent output stability under an applied electric field are crucial for high-precision positioning actuator applications [1,2]. To meet the need for practical application, piezoelectric single crystals such as $Pb(Mg_{1/3}Nb_{2/3})O_3$–$PbTiO_3$ (PMN–PT), $Pb(Mg_{1/3}Nb_{2/3})O_3$–$PbZrO_3$–$PbTiO_3$ (PMN–PZ–PT), and $Pb(Mg_{1/3}Nb_{2/3})O_3$–$Pb(In_{1/2}Nb_{1/2})O_3$–$PbTiO_3$ (PMN–PIN–PT) have been widely investigated due to their ultra-high piezoelectric coefficient ($d_{33} > 1400$ pC/N) and electromechanical coupling factor ($k_p \approx 0.9$) [3–6]. However, the production of single crystals is quite demanding in terms of manufacturing cost, controlling the homogeneity of the composition, and limited shapes and sizes [7,8].

Crystallographically textured piezoceramics, fabricated through the templated grain growth (TGG) method, emerge as promising alternatives [7–10]. They offer comparable unipolar strain to single crystals and improved mechanical strength, along with versatility in shapes and sizes [7–10]. However, these textured piezoceramics exhibit notable strain hysteresis compared to single crystals [11]. This hysteresis, which is related to ferroelectric domain wall movement, is influenced by external factors, such as electric field and temperature, as well as internal factors like stress, grain boundary, and defects [1,12–15].

As hysteresis can impede the material's applicability for precise positioning, it has been the subject of several studies [11,16–18]. One key aspect of this hysteresis is the persistence of remanent strain (S_r) after removing the electric field, affecting the consistency of subsequent strain cycles [19]. The duration S_r remains in the material, termed relaxation time, is therefore crucial for achieving consistency in strain responses and remains an area that requires investigation. The time delay for S_r relaxation may vary for different material systems due to differences in domain wall motion, which depends on the material's nature and microstructure. In terms of the material's nature, domain wall motion is related to the coercive field (E_C); materials with higher E_C have more difficulty in domain wall motion [20]. As a result, materials with higher E_C may require a longer relaxation time than those with lower E_C [20–22]. In terms of microstructure, the grain boundary in polycrystalline ceramics can impede domain wall motion, leading to a longer relaxation time [12–15]. For textured piezoceramics, embedded templates can impede domain wall motion, further increasing the relaxation time [7,11,23]. For the single crystals, the relaxation time is expected to be short because there are no grain boundaries and embedded templates.

* Corresponding author at: Faculty of Mechanical Engineering and Ship Technology, Gdansk University of Technology, 80-233 Gdansk, Poland.
E-mail address: jaejeon@pg.edu.pl (J.-H. Jeon).

https://doi.org/10.1016/j.rinp.2024.108007
Received 22 July 2024; Received in revised form 17 September 2024; Accepted 7 October 2024
Available online 10 October 2024

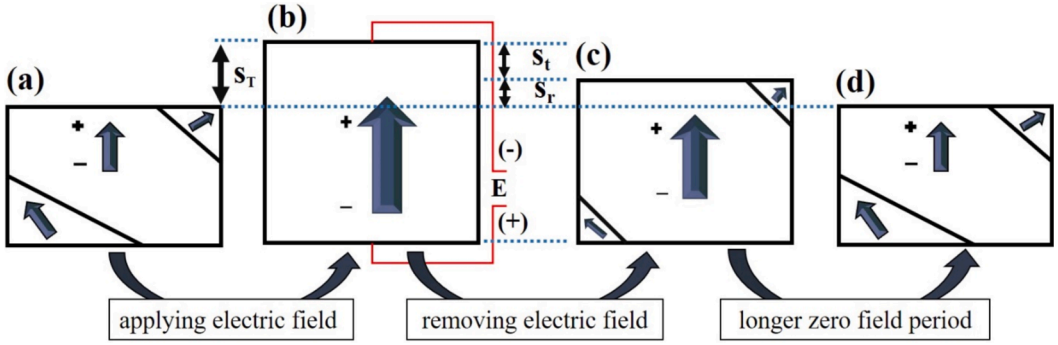

Fig. 1. Model representation of domain reorientation of poled ceramics (a), under electric field (b), immediately after removing electric field (c), and after a longer zero-field period (d). S_T: total strain, S_t: true strain, S_r: remanent strain.

Recently, we have reported excellent electric-field induced strain and high $T_C > 230$ °C obtained from textured 0.4PMN–0.22PZ–0.38PT and 0.37PMN–0.29PIN–0.34PT piezoceramics [24–26]. These textured piezoceramics are currently under consideration to be used for piezo-pumps to replace the mechanical pump installed in loop heat pipes operating at intermediate temperatures. The role of the mechanical pump is to prevent the occurrence of dry-out of the working fluid in the evaporator and achieve stable start-up of the loop heat pipes by supplying an optimal amount of additional working fluid to the evaporator. Because the mechanical pump is usually bulky and complex [27,28], the piezo-pump with simple and small sizes is expected to be a promising candidate to replace it. The amount of the working fluid supplied by the piezo-pump can be accurately controlled due to the precision positioning characteristic of the piezoceramics. This paper investigates the impact of embedded templates on S_r relaxation time in textured 0.4PMN–0.22PZ–0.38PT and 0.37PMN–0.29PIN–0.34PT piezoceramics for precision positioning applications. By comparing the relaxation time of the textured piezoceramics with those of their non-textured counterparts and single crystal PMN–PT, we aim to understand how microstructure influences S_r relaxation time and consequent strain response, offering insights for optimizing piezoceramics in precision positioning applications.

Experimental

High-purity powders of PbO (≥99.9 %, Aldrich, USA), $MgNb_2O_6$ (H. C. Strack, Germany), ZrO_2 (99 %, Aldrich, Germany), TiO_2 (99.8 %, Aldrich, Canada), In_2O_3 (99.99 %, Aldrich, USA), Nb_2O_5 (99.9 % Aldrich, China), Bi_2O_3 (99.9 %, Aldrich, Germany), $BaCO_3$ (≥99.0 %, Aldrich, USA), NaCl (≥99 %, Aldrich, USA), and KCl (≥99 %, Aldrich, USA) were used as raw materials.

The 0.4PMN–0.22PZ–0.38PT matrix powder was synthesized by solid-state reaction processing. Stoichiometric amounts of PbO, ZrO_2, TiO_2, and $MgNb_2O_6$ powders were mixed in ethanol by conventional ball milling for 24 h using a polyethylene bottle and yttria-stabilized ZrO_2 (YSZ) balls. This mixture was then dried and calcined at 900 °C for 1 h, after which the calcined powder was subjected to planetary ball milling for 50 h to reduce the particle size. The 0.37PMN–0.29PIN–0.34PT matrix powder was synthesized *via* a two-step columbite precursor method [29]. To synthesize $InNbO_4$ powder, stoichiometric amounts of In_2O_3 and Nb_2O_5 powders were mixed by ball-milling for 24 h; following, the mixture was calcined at 925 °C for 6 h in a box furnace. To synthesize 0.37PMN–0.29PIN–0.34PT matrix powder, stoichiometric amounts of PbO, TiO_2, $MgNb_2O_6$, and pre-synthesized $InNbO_4$ powders were mixed by ball-milling again for 24 h and then calcined at 850 °C for 6 h.

The plate-like $BaTiO_3$ (BT) template was prepared via molten-salt synthesis followed by a topochemical microcrystal conversion process. A stoichiometric mixture of Bi_2O_3 and TiO_2 (2:3 M ratio) was heat-treated in a salt (NaCl + KCl mixture, 1:1 M ratio) at 1000 °C for 1 h to obtain a plate-like $Bi_4Ti_3O_{12}$ (BiT) precursor. Then a mixture of the BiT precursor and $BaCO_3$ (1:5 M ratio) was heat-treated again in the same salt at 1000 °C for 1 h to synthesize the BT platelets. From the as-synthesized BT platelets, the majority of BT particles smaller than 5 μm were removed utilizing a simple sedimentation technology and the residual BT platelets were used as the template for texturing.

Green compacts of 0.4PMN–0.22PZ–0.38PT and 0.37PMN–0.29PIN–0.34PT piezoceramics were prepared by tape-casting using 5 and 3 vol% of BT templates, respectively, followed by lamination, debinding, and cold-isostatic pressing. Finally, textured

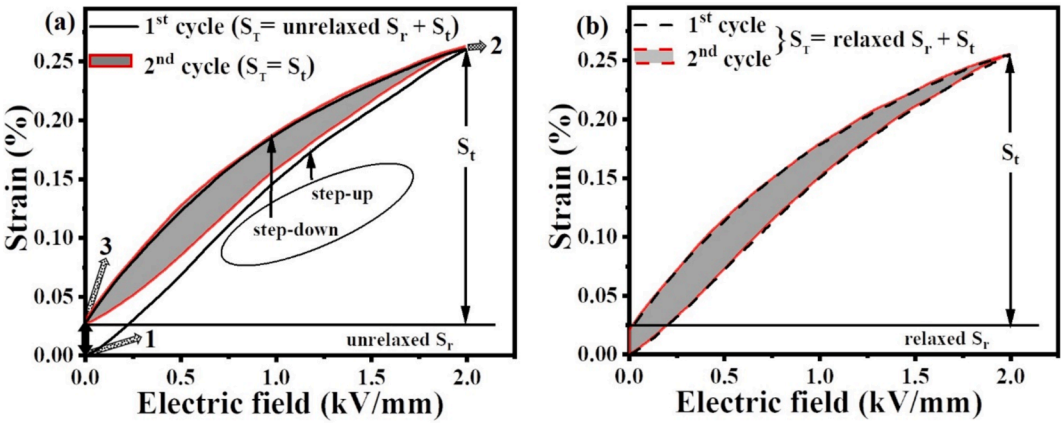

Fig. 2. Unipolar strain response of textured 0.4PMN–0.22PZ–0.38PT ceramics at 2 kV/mm for the first and second cycles in a continuous operation (a) and in a discontinuous operation with a 1 s delay between the cycles (b).

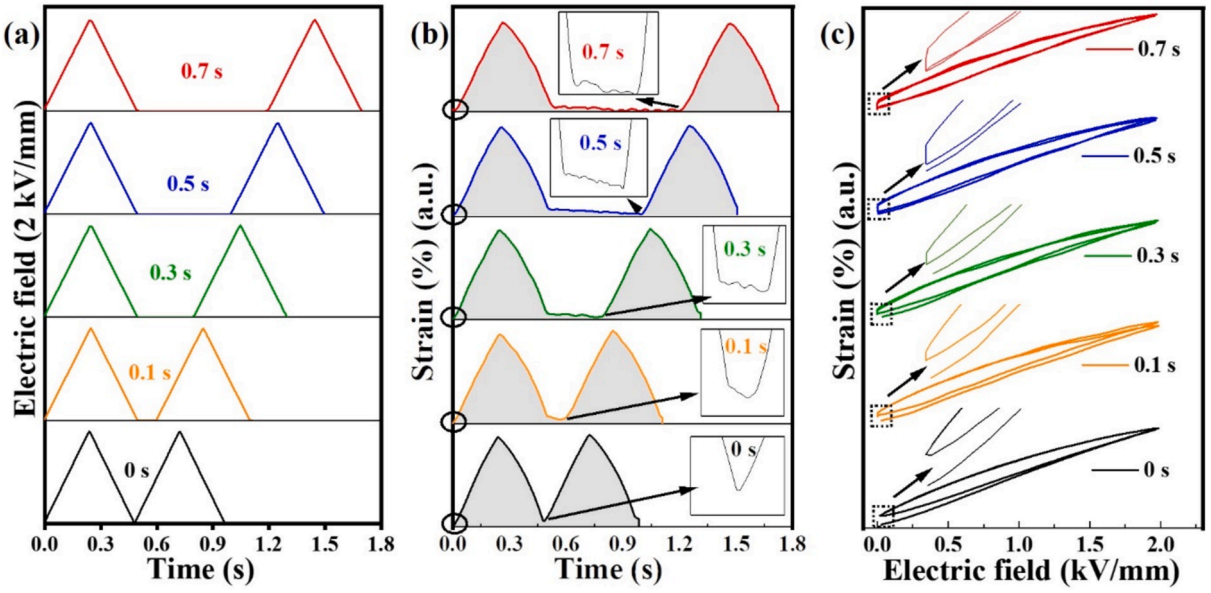

Fig. 3. Electric field profiles with 0 to 0.7 s delays between the first and second cycles applied to textured 0.4PMN–0.22PZ–0.38PT (a) and unipolar strain response of the first and second cycles (b), (c).

0.4PMN–0.22PZ–0.38PT and 0.37PMN–0.29PIN–0.34PT piezoceramics were manufactured by sintering the green compacts at 1200 and 1175 °C for 10 h, respectively. Details of the matrix powder preparation, BT template synthesis and sedimentation, and tape-casting process are given in our previous papers [24–26].

For comparison, non-textured piezoceramics of both compositions were prepared by sintering at the same temperatures and time. A commercial PMN–PT single crystal, provided by Quintes (Korea), was also utilized for an additional comparison. For electromechanical analysis, a silver paste was printed on both sides of disc-shaped samples and fired at 650 °C for 30 min. The samples were poled by applying a direct current (DC) field of 3 kV/mm for 30 min in a silicone oil bath at 120 ℃. A laser displacement sensor (aixACCT Systems GmbH 2013, Germany) was used to analyze the field-induced polarization and unipolar strain response.

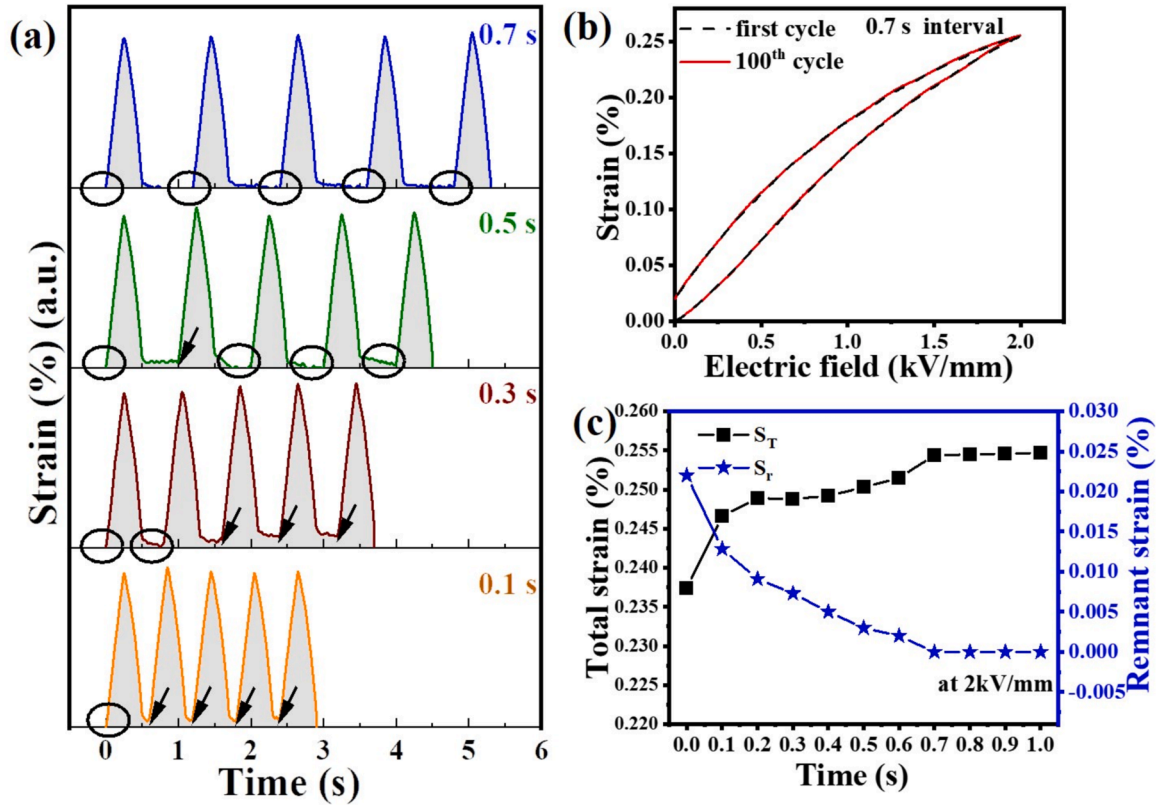

Fig. 4. Five successive strain cycles of textured 0.4PMN–0.22PZ–0.38PT with 0.1 to 0.7 s delays between cycles (a), a comparison of the first and hundredth strain cycles with a 0.7 s delay (b), and S_T and S_r versus time delay between cycles (c).

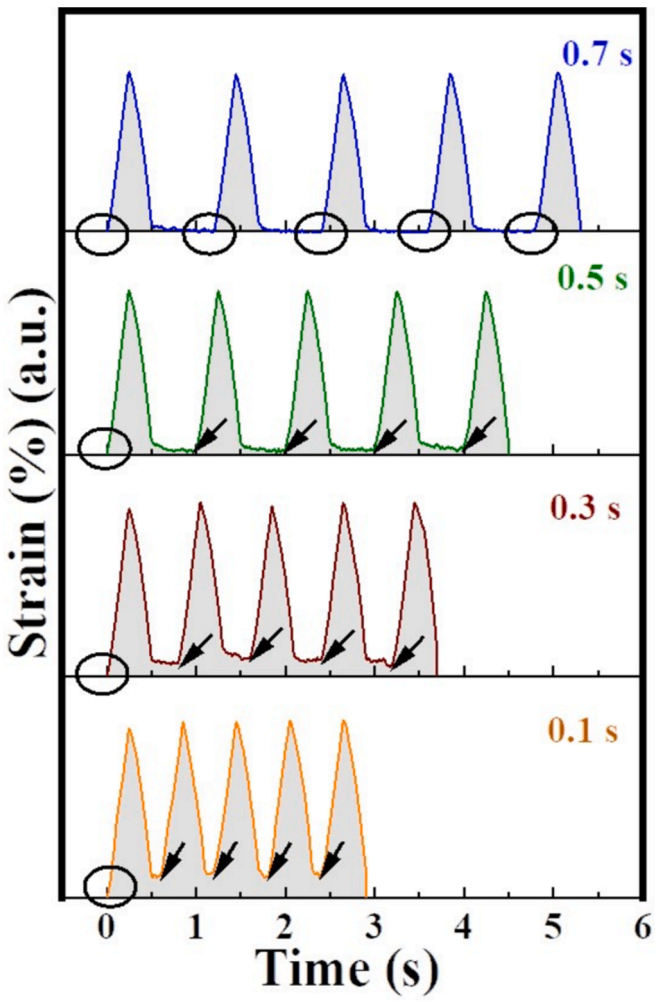

Fig. 5. Five successive strain cycles of non-textured 0.4PMN–0.22PZ–0.38PT with 0.1 to 0.7 s delays.

Result and discussion

Time delay required for remanent strain relaxation in textured and non-textured 0.4PMN–0.22PZ–0.38PT piezoceramics

When an electric field is applied above the E_C of ferroelectric materials, the domains align to the level of saturation along the direction of the field, resulting in total strain (S_T) in the material, as shown in Fig. 1 (a) to (b) [30]. When the external electric field is removed, the aligned domains depolarize slightly but do not return immediately to their original position, resulting in a remanent strain (S_r), as shown in Fig. 1 (b) to (c) [30]. For an extended zero-field period, as shown in Fig. 1(c) to (d), the depolarization may continue until the S_r is fully relaxed. The rate of this depolarization can be affected by point defect dipoles, grain boundaries, pores, etc. that impede domain wall motion, leading to longer relaxation time [12,13,31–35].

Fig. 2(a) shows the unipolar strain response of textured 0.4PMN–0.22PZ–0.38PT piezoceramics containing 5 vol% BT templates measured at 2 kV/mm for the first and second cycles in continuous operation, with a delay set to 0 s. In the first cycle, when the applied field is dropped to zero, the strain remains at a higher level (3) than its starting point (1). The second cycle starts from the endpoint of the first cycle (3) due to unrelaxed S_r. For the first cycle, the S_T is therefore the sum of unrelaxed S_r and the true strain (S_t), while for the second cycle, S_T equals S_t. In discontinuous operation, with delay > 0 s, the second cycle was measured 1 s after the first cycle. For both the first and second cycles, S_T is equal, as shown in Fig. 2(b), indicating that S_r fully relaxed in 1 s and the relaxation time therefore is $\leq$1 s.

To determine the minimum time delay for achieving full S_r relaxation in the textured 0.4PMN–0.22PZ–0.38PT piezoceramics, the first and second strain cycles were measured with $\leq$1 s delay, as shown in Fig. 3. Fig. 3(a) shows the applied electric field waveforms with various delay intervals between the first and second cycles. It can be observed from Fig. 3(b) and (c) that the gap between the starting point of the first cycle, indicated by the ring, and the second cycle, indicated by the arrow, gradually decreases as the delay between pulses increases. Eventually, the gap disappears at 0.7 s delay, indicating that S_r fully relaxes and therefore the first and second strain cycles are identical.

To investigate the consistency of the S_T level, five successive cycles were measured with 0.1, 0.3, 0.5, and 0.7 s delays between the cycles, as shown in Fig. 4(a). For the 0.1 s delay, compared to the starting point of the first strain cycle (indicated by the ring), the starting points of the following strain cycles are at a higher level (indicated by the arrow). At 0.3 and 0.5 s delays, there is noticeable variability, where some cycles' starting levels align with the first cycle (indicated by the ring), while others differ (indicated by the arrow), indicating that full S_r relaxation is not consistently achieved. However, when the delay is extended to 0.7 s, the starting points of all strain cycles converge, signifying consistent full S_r relaxation between successive cycles and resulting in a stable S_T output. This is confirmed by comparing the first and hundredth strain cycles with a 0.7 s delay, as shown in Fig. 4(b). Further extension of the delay to 0.8, 0.9, and 1 s, as shown in Fig. 4(c), continues to demonstrate consistent S_r and S_T values, highlighting that a delay of 0.7 s or longer is necessary for reliable relaxation.

For the textured 0.4PMN–0.22PZ–0.38PT ceramics, the time delay for achieving full S_r relaxation could be be influenced by the presence of the embedded BT template, the mechanical stress induced by the crystal structure difference between the 0.4PMN–0.22PZ–0.38PT matrix and BT template [8,25], and a slight Ba-ion diffusion within a limited distance from the embedded BT template to the surrounding 0.4PMN–0.22PZ–0.38PT shell of the textured grains [9]. These three factors are expected to hinder the domain wall movement which results in a prolonged time delay for full S_r relaxation.

Non-textured piezoceramics may show a shorter delay to S_r relaxation upon the removal of the applied external field because they do not contain the embedded BT templates. Fig. 5 shows five strain cycles of the non-textured 0.4PMN–0.22PZ–0.38PT piezoceramics measured with 0.1 to 0.7 s delays between cycles. Similar to the textured piezoceramics, the

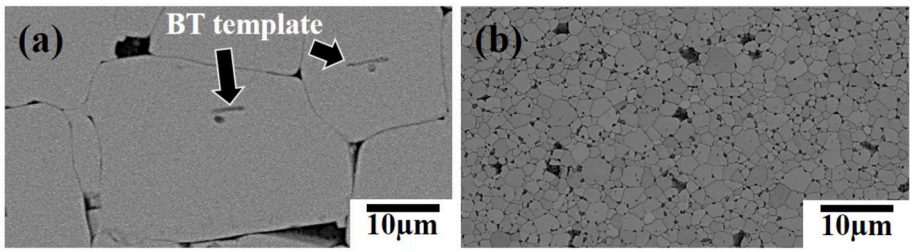

Fig. 6. SEM micrographs of textured (a) and non-textured (b) 0.4PMN–0.22PZ–0.38PT piezoceramics.

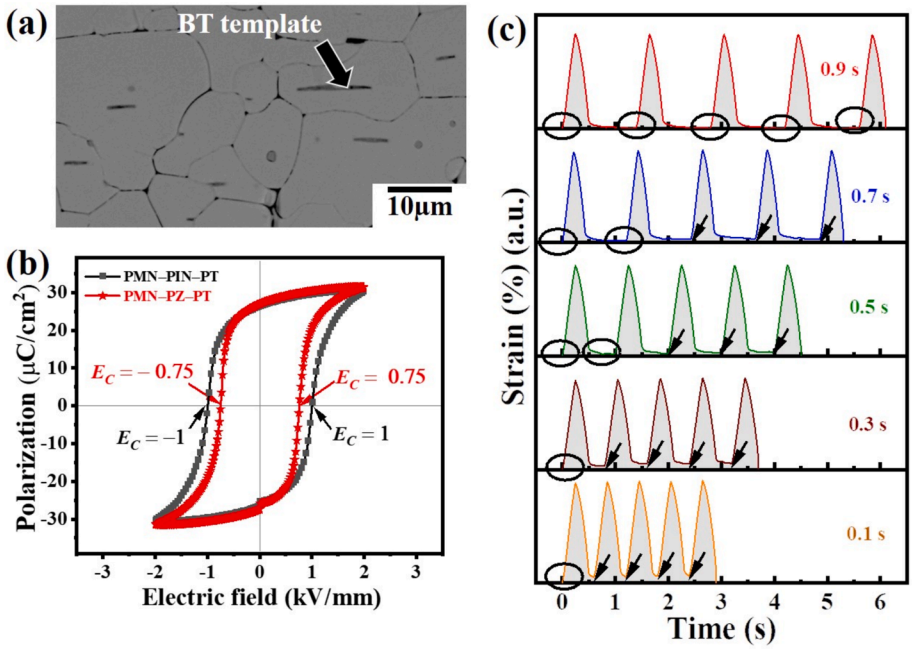

Fig. 7. An SEM micrograph of textured 0.37PMN–0.29PIN–0.34PT piezoceramics (a), P-E loops of textured 0.4PMN–0.22PZ–0.38PT and 0.37PMN–0.29PIN–0.34PT piezoceramics (b), and five successive strain cycles of textured 0.37PMN–0.29PIN–0.34PT piezoceramics with 0.1 to 0.9 s delays (c).

non-textured piezoceramics also exhibit decreasing S_r with increasing delay. Eventually, the S_r drops to zero between successive cycles with a 0.7 s delay, resulting in a consistent level of S_T output. Despite the relatively shorter delay for S_r relaxation expected for the non-textured piezoceramics owing to the absence of the embedded BT template, the relaxation time was the same as that obtained in the textured piezoceramics.

This can be explained by examining the grain size difference between the textured 0.4PMN–0.22PZ–0.38PT with an average grain size of 23 μm and the non-textured counterpart with an average grain size of 4 μm, as depicted in Fig. 6. The significant grain size difference between the textured (0.4PMN–0.22PZ–0.38PT) ceramics and the non-textured counterpart can be attributed to the use of TGG in the textured ceramics, which promotes anisotropic grain growth and results in larger grains. In contrast, the non-textured ceramics, processed without templating, exhibit smaller grains due to the absence of such directed growth, as explained in our previous work [26]. This is because the domain wall can be pinned by the grain boundary and the intensity of pinning depends on the grain boundary area [36–41]. As the grain size becomes smaller, the grain boundary area increases, which possibly results in an increased grain boundary pinning effect on the domain wall [37,41,42]. In addition, because the domain size decreases with the square root of the grain size, domain wall-to-domain wall pinning could also be increased [41–45]. Hence, it can be claimed that the embedded 5 vol% BT templates and the large grains in the textured 0.4PMN–0.22PZ–0.38PT counterbalances the small grains in the non-textured counterpart on the domain wall pinning. This suggests that the time delay for S_r relaxation in the non-textured piezoceramics may not be solely determined by the absence of BT templates, but also by the grain size.

Time delay required for remanent strain relaxation in textured and non-textured 0.37PMN–0.29PIN–0.34PT piezoceramics

Fig. 7(a) shows the microstructure of textured 0.37PMN–0.29PIN–0.34PT piezoceramics, which contains 3 vol% BT templates embedded in the textured grains. Unlike PMN–PZ–PT, PMN–PIN–PT material systems are known for their high E_C, indicating that domain wall motion in this material system is relatively difficult [22,23]. The E_C of the textured 0.37PMN–0.29PIN–0.34PT

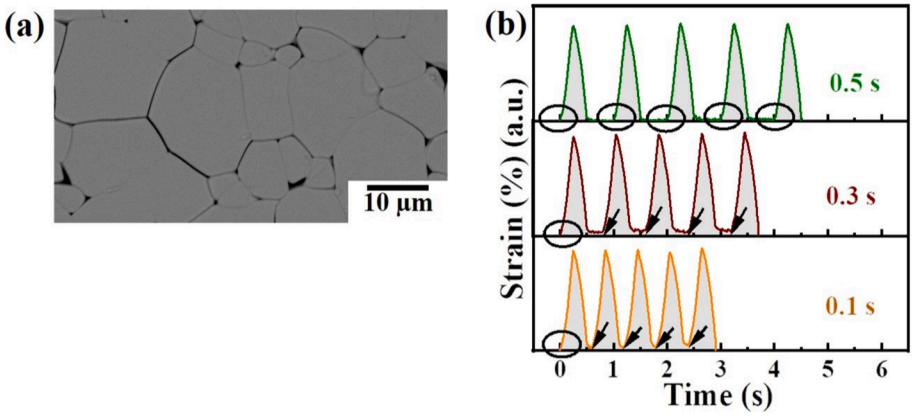

Fig. 8. An SEM micrograph of non-textured 0.37PMN–0.29PIN–0.34PT piezoceramics (a) and five successive strain cycles of non-textured 0.37PMN–0.29PIN–0.34PT piezoceramics with 0.1 to 0.5 s delays (b).

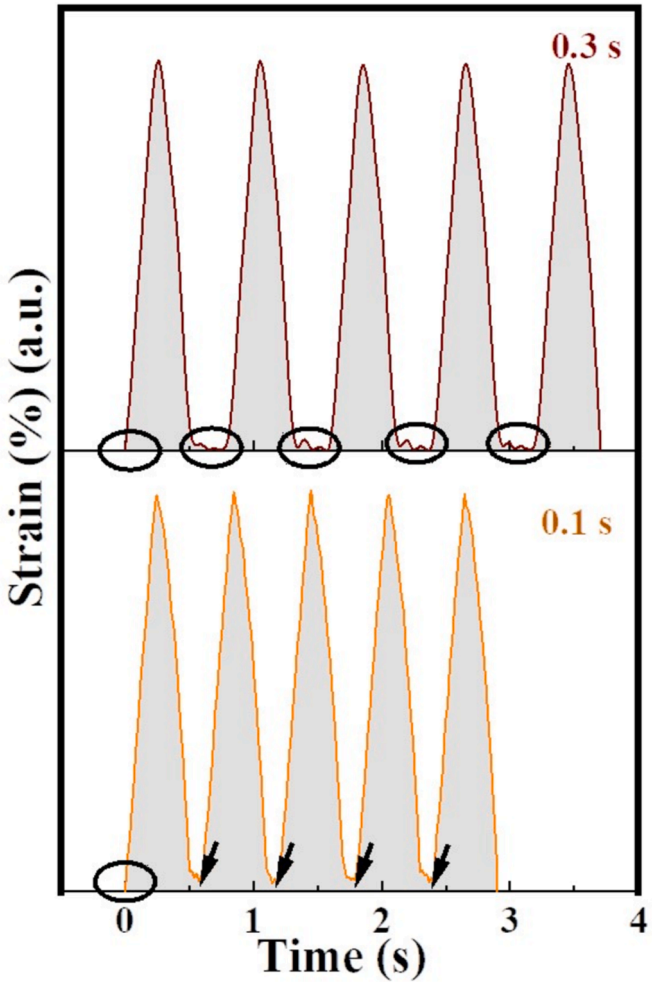

Fig. 9. Five successive strain cycles of PMN–PT single crystal with 0.1 to 0.3 s delays.

piezoceramics is higher than that of the textured 0.4PMN–0.22PZ–0.38PT piezoceramics, as shown in Fig. 7(b). As a result, it is expected that the textured 0.37PMN–0.29PIN–0.34PT piezoceramics will take a longer time delay for S_r relaxation than the textured 0.4PMN–0.22PZ–0.38PT piezoceramics. The relaxation of S_r in the textured 0.37PMN–0.29PIN–0.34PT piezoceramics, as shown in Fig. 7(c), follows a similar trend to that observed in the textured 0.4PMN–0.22PZ–0.38PT piezoceramics. However, complete S_r relaxation takes a longer time delay of 0.9 s likely due to its higher E_C relative to the 0.4PMN–0.22PZ–0.38PT material system.

Fig. 8(a) shows an SEM micrograph of non-textured 0.37PMN–0.29PIN–0.34PT piezoceramics. Compared to the textured 0.37PMN–0.29PIN–0.34PT piezoceramics in Fig. 7(a), the non-textured counterpart in Fig. 8(a) exhibits almost identical average grain size. Therefore, unlike the case in the 0.4PMN–0.22PZ–0.38PT piezoceramics, the grain boundary pinning effect on the domain wall of both the textured and non-textured 0.37PMN–0.29PIN–0.34PT piezoceramics is expected to be nearly the same. As a result, a stronger domain wall pinning is expected in the textured 0.37PMN–0.29PIN–0.34PT ceramics mainly due to the presence of embedded BT templates inside the textured grains. Since there are no templates in the grains of the non-textured 0.37PMN–0.29PIN–0.34PT piezoceramics, a full relaxation of S_r took only 0.5 s as shown in the strain versus time curve in Fig. 8 (b), therefore, it can be said that the longer delay, 0.9 s, for the textured 0.37PMN–0.29PIN–0.34PT ceramics could be due to the effect of embedded BT templates in the textured grains.

Time delay required for remanent strain relaxation in a commercial PMN–PT single crystal

Unlike textured or non-textured piezoceramics, single crystals have no grain boundaries and embedded templates. Consequently, the absence of these features is expected to result in relatively weak pinning of domain walls in single crystals, which may lead to a shorter delay for S_r relaxation compared to textured or non-textured piezoceramics. However, in single crystals, the reorientation of domain walls upon removal of the external field can still be influenced by the presence of local point defect dipoles [46–48]. Fig. 9 displays strain versus time of the single crystal PMN–PT, showing a similar S_r relaxation tendency as the textured and non-textured 0.37PMN–0.29PIN–0.34PT and 0.4PMN–0.22PZ–0.38PT piezoceramics. Despite this, the time delay required for full S_r relaxation for five successive strain cycles of single crystal PMN–PT is 0.3 s. This is much shorter than that required for full S_r relaxation of the textured (0.9 and 0.7 s) and non-textured (0.5 and 0.7 s) 0.37PMN–0.29PIN–0.34PT and 0.4PMN–0.22PZ–0.38PT piezoceramics, respectively. The shorter time delay in the single crystal PMN–PT can be attributed to the absence of grain boundaries and embedded BT templates that pin the domain wall.

Regardless of textured sample, non-textured sample, and single crystal, all relaxation curve showed the decay shape. Further investigation into the decay shape of these relaxation curves is crucial for understanding the creep behavior in ferroelectric materials, which may significantly influence the performance and reliability of piezoelectric devices. To further elucidate the complex domain behaviour in piezoceramics, incorporating computational modelling [49] can be instrumental. Models such as phase-field modelling offer a robust framework for simulating domain formation and evolution under various electrical and mechanical boundary conditions. These models can simulate domain wall motion, domain switching, and intergranular interactions that are critical for interpreting the material's macroscopic electromechanical properties.

In this study, we have explored the relaxation dynamics of remanent strain in textured and non-textured piezoceramics, focusing on the impact of embedded templates and grain sizes. An interesting area for future research is the investigation of how slight variations in template content might influence the relaxation time of real strain, particularly in highly textured ceramics. While our current analysis touches upon this, a more in-depth study could provide valuable insights into optimizing the performance of piezoceramics for specific applications. This could involve both experimental investigations and modeling approaches to understand the microstructural changes induced by varying template concentrations and their effects on domain wall pinning and relaxation dynamics.

Conclusion

We have studied the effect of time delay between electric field pulses on the remanent strain relaxation in textured and non-textured 0.37PMN–0.29PIN–0.34PT and 0.4PMN–0.22PZ–0.38PT piezoceramics and a PMN–PT single crystal. A remanent strain was observed when the time delay between pulses was shorter than each material's characteristic relaxation time. For 0.37PMN–0.29PIN–0.34PT ceramics of comparable grain size, the relaxation time was shorter for the non-textured ceramics, while no difference in the relaxation time could be detected in the 0.4PMN–0.22PZ–0.38PT ceramics where the grain size of the textured ceramics was significantly larger than that of the non-textured counterpart. The PMN–PT single crystal had a shorter relaxation time than all the ceramics. Based on this, we can conclude that both embedded templates and grain boundaries prevent domain reorientation, either by directly pinning the domain walls or by increasing the domain wall density. Therefore, both the microstructure and the time delay between pulses should be carefully controlled to achieve consistent electric field-induced unipolar strain response from not only

lead-based piezoceramics but also lead-free piezoceramics for improved reliability in precision positioning applications.

CRediT authorship contribution statement

Temesgen Tadeyos Zate: Writing – original draft, Methodology, Investigation, Data curation, Conceptualization. **Astri Bjørnetun Haugen:** Writing – review & editing, Funding acquisition. **Dariusz Mikielewicz:** Writing – review & editing, Funding acquisition. **Jae-Ho Jeon:** Writing – review & editing, Writing – original draft, Supervision, Funding acquisition, Conceptualization.

Declaration of competing interest

The authors declare that they have no known competing financial interests or personal relationships that could have appeared to influence the work reported in this paper.

Acknowledgments

We would like to acknowledge financial support from the R&D Convergence Program (CAP-16-09-KITECH) of NST (National Research Council of Science & Technology) of the Republic of Korea, the Nobelium Joining Gdansk Tech Research Community – contract number: DEC 41/2023/IDUB/I.1 of the Poland, and VILLUM FONDEN research grant 37520 of the Denmark.

Data availability

Data will be made available on request.

References

[1] Hu G, Xin W, Zhang M, Chen G, Man J, Tian Y. Development of a fast positioning platform with a large stroke based on a piezoelectric actuator for precision machining. Micromachines 2024;15:1050.
[2] Hao J, Li W, Zhai J, Chen H. Progress in high-strain perovskite piezoelectric ceramics. Mater Sci Eng R Rep 2019;135:1–57.
[3] Yang Z, Qin Z, Zu J. Charging capacitors using single crystal PMN–PT and PZN–PT energy harvesters coupled with the SSHI circuit. Sens Actuators A Phys 2017;266:76–84.
[4] Oh H-T, Lee J-Y, Lee H-Y. Mn-modified PMN–PZT $Pb(Mg_{1/3}Nb_{2/3})O_3$–$Pb(Zr, Ti)_O3$ single crystals for high power piezoelectric transducers. J Korean Ceram Soc 2017;54(2):150–7.
[5] Li F, Zhang S, Lin D, Luo J, Xu Z, Wei X, et al. Electromechanical properties of $Pb(In_{1/2}Nb_{1/2})O_3$–$Pb(Mg_{1/3}Nb_{2/3})O_3$–$PbTiO_3$ single crystals. J Appl Phys 2011;109(1):014108.
[6] Sun E, Zhang R, Wu F, Cao W. Complete matrix properties of [001]c and [011]c poled $0.33Pb(In_{1/2}Nb_{1/2})O_3$–$0.38Pb(Mg_{1/3}Nb_{2/3})O_3$–$0.29PbTiO_3$ single crystals. J Alloys Compd 2013;553:267–9.
[7] Messing GL, Trolier-McKinstry S, Sabolsky EM, Duran C, Kwon S, Brahmaroutu B, et al. Templated grain growth of textured piezoelectric ceramics. Crit Rev Solid State Mater Sci 2004;29(2):45–96.
[8] Liu H, Li X, Xing Z, Mi Q, Shi T, Zhou X, et al. Research progress in the study of textured piezoelectric ceramics. Mater Sci Technol 2024. 02670836241272079.
[9] Yan Y, Cho KH, Priya S. Piezoelectric properties and temperature stability of Mn-doped $Pb(Mg_{1/3}Nb_{2/3})$–$PbZrO_3$–$PbTiO_3$ textured ceramics. Appl Phys Lett 2012;100(13):132908.
[10] Yan Y, Cho KH, Maurya D, Kumar A, Kalinin S, Khachaturyan A, et al. Giant energy density in [001]-textured $Pb(Mg_{1/3}Nb_{2/3})O_3$–$PbZrO_3$–$PbTiO_3$ piezoelectric ceramics. Appl Phys Lett 2013;102(4):042903.
[11] Setter N. Piezoelectric Materials in Devices: Extended Reviews on Current and Emerging Piezoelectric Materials, Technology, and Applications. Ceramics Laboratory, EPFL Swiss Federal Institute of Technology; 2002.
[12] Taylor DV, Damjanovic D. Domain wall pinning contribution to the nonlinear dielectric permittivity $InPb(Zr, Ti)_O3$ thin films. Appl Phys Lett 1998;73(14):2045–7.
[13] S. Trolier-McKinstry, N. Bassiri Gharb, D. Damjanovic, Piezoelectric Nonlinearity Due to Motion of 180 Domain Walls in Ferroelectric Materials at Subcoercive Fields: A Dynamic Poling Model, Appl. Phys. Lett. 2006. 88 (20) (2006) 202901.
[14] Damjanovic D, Demartin M. The rayleigh law in piezoelectric ceramics. J Phys d: Appl Phys 1996;29(7):2057.
[15] Setter N, Damjanovic D, Eng L, Fox G, Gevorgian S, Hong S, et al. Ferroelectric thin films: review of materials, properties, and applications. J Appl Phys 2006;100(5):051606.
[16] G. Bertotti, I.D. Mayergoyz, Eds, The Science of Hysteresis: Physical Modeling, Micromagnetics, and Magnetization Dynamics, GPP, (2) (2006).
[17] Hall D. Review nonlinearity in piezoelectric ceramics. J Mater Sci 2001;36(19):4575–601.
[18] Park S-E, Shrout TR. Ultrahigh strain and piezoelectric behavior in relaxor based ferroelectric single crystals. J Appl Phys 1997;82(4):1804–11.
[19] Kungl H, Fett T, Wagner S, Hoffmann MJ. Nonlinearity of strain and strain hysteresis in morphotropic lasr-doped lead zirconate titanate under unipolar cycling with high electric fields. J App Phys 2007;101(4):044101.
[20] Tian J, Han P. Growth and characterization on PMN–PT based single crystals. Crystals 2014;4(3):331–41.
[21] Li X, Wang Z, He C, Long X, Ye ZG. Growth and piezo-/ferroelectric properties of PIN–PMN–PT single crystals. J Appl Phys 2012;111(3):034105.
[22] Zhang S, Li F, Sherlock NP, Luo J, Lee HJ, Xia R, et al. Recent developments on high curie temperature PIN–PMN–PT ferroelectric crystals. J Cryst Growth 2011;318(1):846–50.
[23] Kwon S, Sabolsky EM, Messing GL, Trolier-McKinstry S. High strain, <001> textured $0.675Pb(Mg_{1/3}Nb_{2/3})O_3$–$0.325PbTiO_3$ ceramics: templated grain growth and piezoelectric properties. J Am Ceram Soc 2005;88(2):312–7.
[24] Kim M, Upadhyay A, Lim K-W, Zate TT, Jeon J-H. Optimisation of matrix composition for texturing of morphotropic phase boundary $Pb(Mg_{1/3}Nb_{2/3})O_3$–$PbZrO_3$–$PbTiO_3$ piezoelectric ceramics using $BaTiO_3$ template. J Eur Ceram Soc 2021;41:7639–44.
[25] Zate TT, Ko N-R, Yu H-L, Sun J-W, Jo W, Jeon J-H. Textured $Pb(Mg_{1/3}Nb_{2/3})O_3$–$Pb(In_{1/2}Nb_{1/2})O_3$–$PbTiO_3$ ceramics with enhanced piezoelectric properties and high curie temperature prepared by low-temperature sintering. Sens Actuator A Phys 2024;366:114929.
[26] Zate TT, Kim M, Jeon J-H. Outstanding unipolar strain of textured $Pb(Mg_{1/3}Nb_{2/3})O_3$–$PbZrO_3$–$PbTiO_3$ piezoelectric ceramics manufactured by particle size distribution control of the plate-like $BaTiO_3$ template. Sens Actuator A Phys 2022;335:113373.
[27] Guo H, Ji X, Xu J. Research and development of loop heat pipe – a review. Front. Heat Mass Transfer 2020;14:14.
[28] Setyawan I, Putra N, Hakim II. Experimental investigation of the operating characteristics of a hybrid loop heat pipe using pump assistance. Appl Thermal Eng 2018;130:10–6.
[29] Chang Y, Watson B, Fanton M, Meyer Jr RJ, Messing GL. Enhanced texture evolution and piezoelectric properties in CuO-Doped $Pb(In_{1/2}Nb_{1/2})O_3$–$Pb(Mg_{1/3}Nb_{2/3})O_3$–$PbTiO_3$ grain-oriented ceramics. Appl Phys 2017;111:232901.
[30] Zhao D, Lenz T, Gelinck GH, Groen P, Damjanovic D, de Leeuw DM, et al. Depolarization of multidomain ferroelectric materials. Nat Commun 2019;10(1):1–11.
[31] D.M. Marincel, The Influence of Crystal Defects on Domain Wall Motion in Thin Film $Pb(Zr,Ti)O_3$, PSU (2014).
[32] Gao P, Nelson CT, Jokisaari JR, Baek SH, Bark CW, Zhang Y, et al. Revealing the role of defects in ferroelectric switching with atomic resolution. Nat Commun 2011;2(1):1–6.
[33] Pramanick A, Damjanovic D, Nino JC, Jones JL. Subcoercive cyclic electrical loading of lead zirconate titanate ceramics I: nonlinearities and losses in the converse piezoelectric effect. J Am Ceram Soc 2009;92(10):2291–9.
[34] Chang L, McMillen M, Gregg J. The influence of point defects and inhomogeneous strain on the functional behavior of thin film ferroelectrics. Appl Phys Lett 2009;94(21):212905.
[35] Nelson CT, Gao P, Jokisaari JR, Heikes C, Adamo C, Melville A, et al. Domain dynamics during ferroelectric switching. Sci 2011;334(6058):968–71.
[36] Marincel DM, Zhang H, Kumar A, Jesse S, Kalinin SV, Rainforth WM, et al. Piezoelectrics: influence of a single grain boundary on domain wall motion in ferroelectrics. Adv Funct Mater 2014;24(10):1408.
[37] Randall CA, Kim N, Kucera JP, Cao W, Shrout TR. Intrinsic and extrinsic size effects in fine-grained morphotropic phase boundary lead zirconate titanate ceramics. J Am Ceram Soc 1998;81(3):677–88.
[38] Ihlefeld JF, Vodnick AM, Baker SP, Borland WJ, Maria JP. Extrinsic scaling effects on the dielectric response of ferroelectric thin films. J Appl Phys 2008;103(7):074112.
[39] Damjanovic D, Demartin M. Contribution of the irreversible displacement of domain walls to the piezoelectric effect in barium titanate and lead zirconate titanate ceramics. J Condens Matter Phys 1997;9(23):4943.
[40] Demartin M, Damjanovic D. Dependence of the direct piezoelectric effect in coarse and fine grain barium titanate ceramics on dynamic and static pressure. Appl Phys Lett 1996;68(21):3046–8.
[41] Griggio F, Trolier-McKinstry S. Grain size dependence of properties in lead nickel niobate-lead zirconate titanate films. J Appl Phys 2010;107(2):024105.
[42] Choudhury S, Li YL, Krill Iii C, Chen LQ. Effect of grain orientation and grain size on ferroelectric domain switching and evolution: phase field simulations. Acta Mater 2007;55(4):1415–26.
[43] Cao W, Randall CA. Grain size and domain size relations in bulk ceramic ferroelectric materials. J Phys Chem Solids 1996;57(10):1499–505.
[44] Arlt G, Hennings D, De With G. Dielectric properties of fine-grained barium titanate ceramics. J Appl Phys 1985;58(4):1619–25.
[45] Marincel DM, Zhang H, Jesse S, Belianinov A, Okatan MB, Kalinin SV, et al. Domain wall motion across various grain boundaries in ferroelectric thin films. J Am Ceram Soc 2015;98(6):1848–57.
[46] Yang TJ, Gopalan V, Swart PJ, Mohideen U. Direct observation of pinning and bowing of a single ferroelectric domain wall. Phys Rev Lett 1999;82(20):4106.

[47] Yang C, Sun E, Yang B, Cao W. Theoretical study on local domain pinning effect due to defect dipole alignment. J Phys d: Appl Phys 2018;51(41):415303.
[48] Kim Y, Han H, Vrejoiu I, Lee W, Hesse D, Alexe M. Origins of domain wall pinning in ferroelectric nanocapacitors. Nano Converg 2014;1(1):1–6.
[49] Arockiarajan A, Menzel A, Delibas B, Seemann W. Computational modeling of rate-dependent domain switching in piezoelectric materials. Eur J Mech A Solids 2006; 25(6):950–64.

Temesgen Tadeyos Zate is a postdoctoral researcher at Department of Energy Conversion and Storage at the Technical University of Denmark (DTU). His current research interests are lead-based and lead free piezoelectric ceramics, textured ceramics and single crystals.

Astri Bjørnetun Haugen is an Associate Professor at Department of Energy Conversion and Storage at the Technical University of Denmark (DTU). Her current research interests are lead-free piezoelectric ceramics, oxygen membranes, texture and microstructure control in ceramics.

Dariusz Mikielewicz is a Professor at the Gdansk University of Technology, Poland. His current research interests are thermodynamics and heat transfer, heat technology, energy systems, and piezo-pump.

Jae-Ho Jeon is a Professor at the Gdansk University of Technology, Poland. His research interests are interfacial phenomena, sintering, grain growth, and texturing of piezoelectric ceramics.